JCTC Journal of Chemical Theory and Computation

Article

pubs.acs.org/JCTC

Calculating Off-Site Excitations in Symmetric Donor−Acceptor Systems via Time-Dependent Density Functional Theory with Range-Separated Density Functionals

Heidi Phillips, Eitan Geva,* and Barry D. Dunietz*,†

Department of Chemistry, University of Michigan, Ann Arbor, Michigan, United States

Supporting Information

ABSTRACT: Time-dependent density functional theory with range-separated hybrid functionals is used to calculate off-site excitations involving transitions between spatially separated orbitals in weakly coupled systems. Although such off-site excitations involve charge transfer, orbital degeneracy in symmetrical systems results in linear combinations of off-site excitations with equal weights and therefore zero net charge-transfer character. Like other types of off-site excitations, such "hidden" charge-transfer excitations are not accurately captured by conventional density functionals. We show that the recently introduced Baer−Neuhauser−Livshitz range-separated hybrid functional accurately characterizes such hidden off-site excitation energies via applications to the ethene dimer model system and to dye-functionalized silsesquioxanes.

1. INTRODUCTION

Organic materials offer viable, low-cost alternatives to crystalline semiconductors in optoelectronic applications, such as organic photovoltaic (OPV) and organic light-emitting diode (OLED) devices.[1−5] Systematically improving the performance and efficiency of such OPV and OLED devices calls for detailed molecular understanding of the underlying charge-separated states and charge-transfer (CT) processes. Since a purely experimental characterization of these states and processes is difficult, it is beneficial to use theoretical modeling and ab initio calculations for this purpose.

Time-dependent density functional theory (TDDFT) has become a widely used tool for characterizing excited electronic states.[6−8] However, while TDDFT is formally exact, its conventional implementations suffer from well-documented limitations in treating CT excitations.[9−14] Not only do conventional implementations fail to accurately capture the correct asymptotic distance dependence of the electron−hole Coulomb interaction, but the actual orbital energies are often found to be underestimated due to the derivative discontinuity.[15−23]

Previously, conventional TDDFT was shown to underestimate off-site excitation energies even when no net transfer of charge is involved.[24−26] For instance, a previous study considered the low-lying $\pi-\pi^*$ excitations in a symmetric ethene (C_2H_4) dimer system, which correspond to the transition between the monomer highest occupied and lowest unoccupied molecular orbitals, HOMO and LUMO, respectively.[24−26] Four excitations were observed: two on-site excitations, which were localized on each monomer, and two off-site excitations, which each involve CT from the HOMO of one ethene to the LUMO[27] of the other (see Figure 1). In this case, the CT due to the off-site excitations is vanishing when the two states are assigned equal weights. The two states are degenerate due to the system symmetry. We point out that the MO representation is arbitrary and can be chosen to be localized on each monomer (as shown in Figure 1) or delocalized over the dimer, that is, written as symmetrical and antisymmetrical linear combinations with equal weights for the monomer-localized orbitals.[28] We emphasize that in either of the two possible MO representations, localized and delocalized, we obtain pairs of equivalent excited states (further discussed in the Supporting Information). In the delocalized representation, each of the two states are of non-CT character, whereas in the

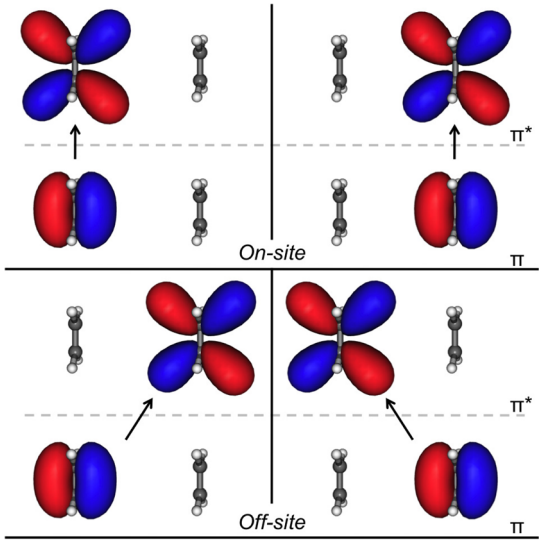

Figure 1. The four possible $\pi-\pi^*$ excitations of the ethene dimer. The two on-site excitations and two off-site excitations are shown in the top and bottom panels, respectively. Orbital degeneracy in symmetric dimers allows the excitations to be written also as linear combinations of the individual off-site excitations pictured above, which can conceal the underlying CT nature evidenced in the localized MO representation.

Received: April 20, 2012
Published: June 5, 2012

localized representation, each of the states exhibit CT character and are mirror images of each other. Though the degenerate off-site excitations in a symmetric dimer possess zero net CT, due to the inherent CT nature of the individual off-site excitations, their energies are poorly described by conventional TDDFT.

In this paper, we demonstrate the ability of range-separated hybrid (RSH) functionals to correctly treat off-site CT excitations. Our aim is 2-fold:

(1) We demonstrate that the shortcomings of conventional functionals in treating off-site CT excitations[24] can be more severe in symmetric systems, characterized by zero net CT. More specifically, we show that a qualitatively correct ordering of the excited electronic energy levels may be accidentally achieved as a result of symmetry-breaking. Thus, conventional functionals may fail in cases involving zero net CT, while they may appear qualitatively correct in cases involving nonzero net CT.

(2) We demonstrate that the Baer−Neuhauser−Livshitz (BNL) RSH functional is able to accurately predict the off-site excitation energies in both the symmetrical and symmetry-broken cases, via applications to the spatially separated model ethene dimer and experimentally relevant dye-functionalized silsesquioxane (SQ). In a previous study, the BNL functional was shown to successfully capture off-site excitations between strongly coupled orbitals in oligoacenes.[28] Here we use modes in spatially separated dimer model systems to follow the effect of symmetry breaking on the off-site states' energies.

2. THEORETICAL BACKGROUND

We start, for completeness, by pointing out the origins of CT failures using traditional functionals and emphasize their relations to off-site excitations in symmetric systems. The limitations for treating CT via TDDFT are mainly due to the inability of conventional local exchange−correlation (XC) kernels to account for the distance-dependent exchange contributions when treating transitions between orbitals with zero spatial overlap.[14,24−26,28,29] This failure can be observed by considering the TDDFT eigenvalue problem [in the random phase approximation (RPA)]:[14,28,30,31]

$$\begin{pmatrix} A & B \\ B^* & A^* \end{pmatrix}\begin{pmatrix} X \\ Y \end{pmatrix} = \omega\begin{pmatrix} 1 & 0 \\ 0 & -1 \end{pmatrix}\begin{pmatrix} X \\ Y \end{pmatrix} \tag{1}$$

Here X and Y represent the occupied-to-virtual and virtual-to-occupied contributions to the perturbation density in the molecular orbital representation, and ω is the transition frequency. The matrix elements A and B are given by

$$A_{ia\sigma,jb\tau} = (i_\sigma a_\sigma|r_{12}^{-1}|j_\tau b_\tau) + (1 - c_{HF})(i_\sigma a_\sigma|f_{\sigma\tau}|j_\tau b_\tau) - c_{HF}\delta_{\sigma\tau}(i_\sigma j_\sigma|r_{12}^{-1}|a_\tau b_\tau) + \delta_{\sigma\tau}\delta_{ij}\delta_{ab}(\varepsilon_{a\sigma} - \varepsilon_{i\tau}) \tag{2}$$

$$B_{ia\sigma,jb\tau} = (i_\sigma a_\sigma|r_{12}^{-1}|b_\tau j_\tau) + (1 - c_{HF})(i_\sigma a_\sigma|f_{\sigma\tau}|b_\tau j_\tau) - c_{HF}\delta_{\sigma\tau}(i_\sigma b_\sigma|r_{12}^{-1}|a_\tau j_\tau) \tag{3}$$

where i,j and a,b are indices for the ground-state occupied orbitals and virtual orbitals, respectively; σ,τ are the spin indices; r_{12} is the distance between electrons 1 and 2; ε is the orbital energy; c_{HF} is the percentage of Hartree−Fock (HF) exchange included in a hybrid functional; and δ is the Kronecker delta. The nonlocal XC kernel is given by $f_{\sigma\tau}$, though the adiabatic local density approximation is typically applied.

In the case of a transition between spatially separated orbitals (off-site), when a pure density XC functional is used ($c_{HF} = 0$), all terms in A and B vanish for pure CT excitations, except for the last term in A (eq 2), which corresponds to the energy difference between participating orbitals.[14] The resulting CT excitation energies are underestimated due to the lack of distance dependence arising from the Coulomb electron−hole interaction ($\sim -R^{-1}$). When a hybrid XC functional is used, the exchange term in A does not vanish (third term in eq 2), and thus partial distance dependence is captured in the excitation energy. The third term in B (eq 3) will vanish, however, because the spatial overlap will be zero for i,b, and j,a when the spatial overlap is nonzero for i,j and a,b. Although hybrid functionals may partially compensate for some of the discrepancy in off-site excitation energies, the final result usually remains significantly underestimated.

We note that since the B terms in eq 3 vanish for an off-site excitation, the Tamm−Dancoff approximation (TDA)[30,32] equations become equivalent to the full TDDFT. Therefore, for pure CT excitations, TDDFT and TDA predict the same excitation energies.[14,30,32] Importantly, we confirm that these relations hold for the off-site excitations in the symmetric systems that we analyze below in detail.

Another limitation occurs at the ground-state DFT level, where the derivative discontinuity leads to an underestimated energy gap between the Kohn−Sham HOMO and LUMO orbitals. A discontinuity in the derivative of the ground-state energy with respect to particle number, $\partial E/\partial N$, occurs as the particle number crosses an integer value, since the XC potential must "jump" by a constant in order to satisfy the Hohenberg−Kohn theorem.[15,23] The derivative discontinuity, Δ_{XC}, is equal to the difference between the Kohn−Sham HOMO−LUMO gap, $\varepsilon_L - \varepsilon_H$, and the fundamental gap between ionization potential, IP, and electron affinity, EA:

$$\mathrm{IP} - \mathrm{EA} = \varepsilon_L - \varepsilon_H - \Delta_{XC} \tag{4}$$

Calculations using conventional functionals have been shown to lead to a Kohn−Sham HOMO−LUMO gap which is lower than the corresponding fundamental gap.[19,23] Even when hybrid functionals are employed to achieve partial distance dependence, failure to correctly characterize the HOMO−LUMO gap results in underestimated excitation energies between spatially separated frontier orbitals.

Recently developed RSH functionals have been designed to overcome the above-mentioned failures of conventional functionals to account for CT excitations.[21,23,33−44] In RSH functionals, the exchange consists of two terms, one corresponding to long-range (lr) and another to short-range (sr) contributions. This corresponds to writing r^{-1} as a sum of two terms, $r^{-1} \equiv r^{-1}f_{sr}(\gamma r) + r^{-1}f_{lr}(\gamma r)$, where f_{sr} and f_{lr} are complementary switching functions and γ is the so-called range-separation parameter. The short-range exchange is treated with conventional local potentials, such as the local density approximation (LDA) or generalized-gradient approximation (GGA), while the long-range term incorporates exact HF exchange.

RSH functionals address the limitations of TDDFT in treating transitions between spatially separated orbitals. The explicit nonlocal HF exchange in the XC potential, $r^{-1}f_{lr}(\gamma r)$,

prevents the long-range Coulomb interaction term [third term in A (eq 2)] from vanishing.[28] Therefore, when a RSH functional is employed, the matrix element for an off-site excitation with zero spatial overlap between orbitals i and a is given by

$$A^{\mathrm{RSH}}_{ia\sigma,jb\tau}(\text{off-site}) = \delta_{\sigma\tau}\delta_{ij}\delta_{ab}(\varepsilon_{a\sigma} - \varepsilon_{i\tau}) - \delta_{\sigma\tau}(i_\sigma j_\sigma|r_{12}^{-1}f_{\mathrm{lr}}(\gamma r_{12})|a_\tau b_\tau) \quad (5)$$

The excitation energy for transitions between spatially separated orbitals is then equal to the orbital gap minus the distance-dependent Coulomb interaction.

The RSH BNL functional also overcomes limitations associated with the derivative discontinuity by optimizing the range-separation parameter, γ, so as to ensure Koopman's theorem, IP = $-\varepsilon_{\mathrm{H}}$, is satisfied for both the N electron and the $N + 1$ electron systems.[19,28] More specifically, γ is determined by minimizing the following function:

$$J^2(\gamma) = [|\varepsilon_{\mathrm{H}}{}^{\gamma}(N) + \mathrm{IP}^{\gamma}(N)|]^2 + [|\varepsilon_{\mathrm{H}}{}^{\gamma}(N+1) + \mathrm{IP}^{\gamma}(N+1)|]^2 \quad (6)$$

It should be noted that EA(N) is approximately IP($N + 1$), so that IP − EA − ($\varepsilon_{\mathrm{L}} - \varepsilon_{\mathrm{H}}$) is minimized by this procedure, and that calculations performed with an optimal γ were found to yield accurate orbital gaps.[19,23,28] In general, due to corrections in both ground-state DFT and TDDFT formalisms, the BNL functional, as well as other RSH functionals, have been successful at making accurate predictions when applied to several benchmark CT systems.[28,29,36,41,45−53]

3. COMPUTATIONAL METHODS

We begin our analysis by considering the ethene dimer model system previously used to demonstrate the shortcomings of the standard functionals in symmetric systems.[24] We then extend the analysis to the case of functionalized silsesquioxanes. It should be noted that chromophore-functionalized SQs have recently drawn attention due to the ability to tune their optoelectronic properties by the choice of chromophores.[54−57]

Two types of excitations are considered in our study: the on-site low-lying excitations, which are transitions between occupied and unoccupied orbitals localized on the same species, and the corresponding off-site excitations, which are transitions between an occupied orbital localized on one species and an unoccupied orbital localized on the other (see Figure 1). At sufficiently large dimer separation, the on-site excitations coincide with those of the isolated molecules. In the case of symmetric dimers, the off-site excitations have no preference for CT due to orbital degeneracy. We therefore also examine the effect of systematic symmetry-breaking, which removes the degeneracy to reveal the CT nature of these excitations.

In the ethene dimer model, we consider two symmetry-breaking schemes. In one scheme an electric field is applied, and in the other the bond of one ethene is stretched while that of the other ethene remains unchanged. The qualitative effect of these two symmetry-breaking schemes on the orbital gap energies is illustrated in Figure 2. In the case where an electric field is applied, both orbital energies are shifted (i.e., gated) by a similar amount, thereby maintaining almost the same orbital gap. In the case of the bond stretching, the HOMO energy of the stretched ethene increases while the LUMO[27] energy decreases to reduce the orbital gap.

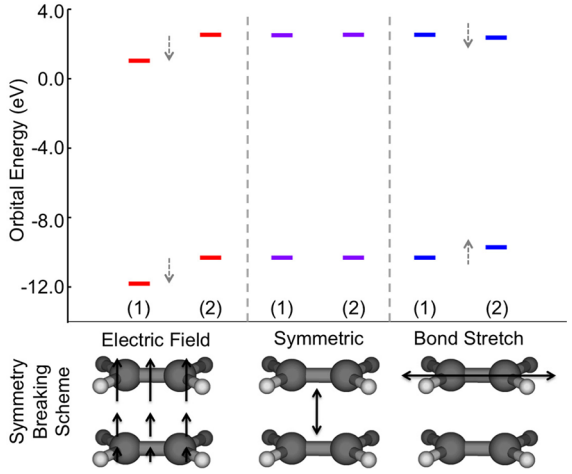

Figure 2. Top: Ethene dimer orbital energies (in electronvolts): (purple) symmetric, (red) symmetry broken by electric field (0.1 V), and (blue) symmetry broken by bond stretching (0.102 Å from equilibrium). The results shown were obtained for a dimer where the ethenes are 15 Å apart, by use of the HF approximation. Bottom: Pictorial description of dimer separation and symmetry-breaking schemes.

All calculations were carried out with a prerelease version of the Q-Chem Program Package version 4.0.[58] The molecular geometry of the ethene monomer was optimized at the B3LYP//cc-pVTZ level of theory. TDDFT calculations on the monomer and dimer systems were performed by use of the aug-cc-pVTZ basis set, with the Slater−Dirac (LDA),[59] PBE (GGA),[60] B3LYP (hybrid),[61−64] and BNL (RSH)[40,41] functionals and the HF approximation. The BNL is a recently developed RSH functional that has been used to successfully treat CT state energies.[28,45−47,65] The range-separation parameter (γ) for the BNL functional was calculated according to eq 6 and was independently determined for each system. The parameter values for the ethene dimer system were centered around 0.40 au, and values for the vinylstilbene−SQ systems were 0.20 au. All values are listed in Table 1 in Supporting Information. All orbitals and densities were visualized via the Molekel program.[66]

4. RESULTS

In this study, we consider the lowest singlet valence excitations corresponding to $\pi-\pi^*$ transitions.[24] The excitation energies and corresponding orbital gaps for the ethene monomer predicted by each functional are listed in Table 1. Importantly, the BNL corresponding orbital gap,[67] 12.4 eV, differs by only 0.1 eV from the fundamental gap, 12.3 eV, which was determined from the experimental IP (10.5 eV) and EA (−1.8 eV) values.[68] The excitation energy predicted by both HF and B3LYP is 7.46 eV. The B3LYP orbital gap of 5.45 eV is

Table 1. Excitation Energy and Corresponding Orbital Gap for Isolated Ethene

XC functional	excitation energy (eV)	orbital gap (eV)
HF	7.46	12.82
BNL	7.59	12.41
B3LYP	7.46	7.37
PBE	6.97	5.58
LDA	7.18	5.63

lower than that predicted by HF and BNL. The PBE and LDA functionals both predict lower excitation energies and orbital gaps than HF and BNL. The orbital gap for the BNL functional is found to be slightly lower than the HF orbital gap; however the BNL excitation energy is slightly higher.

To examine off-site excitations, we consider dimers where the ethenes are separated by 4−15 Å. First, we confirm that at the largest separation distance, 15 Å, the excitation energies and orbital gaps are the same as the corresponding energies of the isolated molecule (orbital energies are included in Table 2 in Supporting Information). We then illustrate the limitations of TDDFT with conventional XC functionals in Figure 3. In this

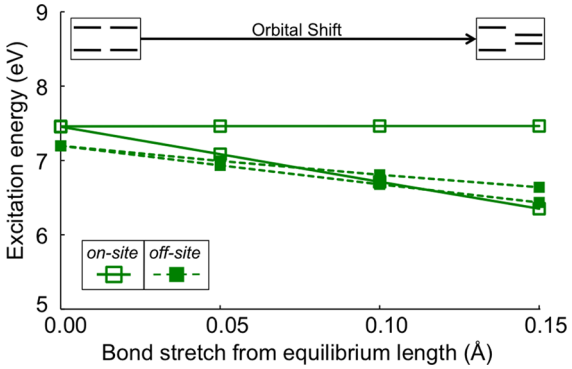

Figure 3. B3LYP excitation energies (in electronvolts) as the bond of one ethene is increasingly stretched at a dimer separation of 15 Å. A schematic illustrating the orbital shift induced by the bond stretching is included to clarify the changes in excitation energies.

case we consider the ordering of the on-site and off-site excitation energies as a function of stretching the C═C bond in one of the ethene molecules. Indeed, as local functionals cannot account for the energy required to separate the electron−hole pair, TDDFT B3LYP underestimates the off-site excitation energies in the symmetric case. The symmetry breaking induced by stretching the bond in one of the ethenes stabilizes the off-site states and even more so the corresponding on-site state (see Figure 3). These trends result in an accidental correct ordering of the off-site excitation energies above the on-site energy for a sufficiently symmetry-broken system.

Importantly, in symmetric systems, the CT nature of off-site excitations can be hidden due to orbital degeneracy. However, these excitation energies remain underestimated within B3LYP. Likewise, in the symmetry-broken dimer, the off-site excitations are obviously CT in nature, but the failure of B3LYP can be hidden by the accidental correct ordering of the excitation energies due to the extent in which the orbital degeneracy is broken. The problem is enhanced as the electronic structure becomes more complex. For example, though the on-site and off-site excitations are clearly designated in the ethene dimer, the assignment is much more difficult in systems such as fully functionalized 8-vinylstilbene−OHSQ.

In the next step, we show that the RSH BNL functional correctly handles off-site excitations in both the symmetric and symmetry-broken ethene dimer. Figure 4a shows both the on-site and off-site excitation energies as a function of dimer separation in a dimer where the bond of one ethene is stretched by 0.102 Å relative to equilibrium. The on-site excitation energies follow the same trends as those of the isolated ethene molecule. However, the off-site excitation energies exhibit quite different trends depending on the XC functional/method.

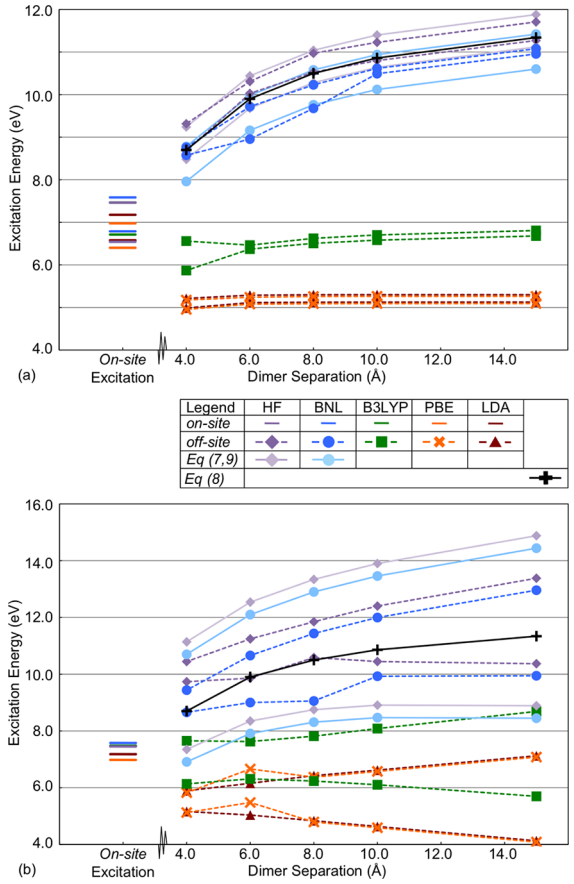

Figure 4. (a) Excitation energies (in electronvolts) when symmetry is broken by bond stretching (0.102 Å from equilibrium) with increasing dimer separation. Off-site energies are compared to eq 7. (b) Excitation energies (in electronvolts) when symmetry is broken by applying a constant electric field with increasing dimer separation. The field (E_f = 0.1 V/Å) is applied at each separation value. Off-site energies are compared to eq 9. For both plots, the off-site energies are also compared to eq 8, the long-range electrostatic interaction limit where experimental IP and EA values are used. On-site energies for the 15 Å separation are included for comparison (Note: HF and B3LYP on-site state energies overlap).

The energies of the off-site excitations should be equal to the orbital gap plus the contribution from the XC kernel. We compare the off-site excitation energies, E_{CT}, to the corresponding orbital gap, $\Delta\varepsilon_{orb}$, minus the Coulomb attraction between the separated charges, $-R^{-1}$ (in atomic units):[24]

$$E_{CT} = \Delta\varepsilon_{orb} - \frac{1}{R} \tag{7}$$

We use the orbital gaps calculated with HF and BNL, since the value of the expression calculated with the orbital gaps of the conventional XC functionals is much lower than the on-site excitation energies. Equation 7 mirrors the long-range electrostatic interaction, where[14,24,26]

$$E_{CT} = \mathrm{IP} - \mathrm{EA} - \frac{1}{R} \tag{8}$$

We present the electrostatic interactions by taking into account the fundamental gap. We use the experimentally determined IP (10.5 eV) and EA (−1.8 eV) energies[68] in order to benchmark the calculated off-site energies with the "experimental trend" in eq 8.

dx.doi.org/10.1021/ct300318g | J. Chem. Theory Comput. 2012, 8, 2661−2668

We find that TDDFT PBE and LDA off-site excitation energies are considerably lower than the on-site excitation energies and do not exhibit correct dependence on the dimer separation distance. The B3LYP energies do depend on dimer separation, but only to the extent that HF exchange is included in the functional. The excitation energy remains underestimated despite including a fraction of HF exchange. On the other hand, the TDHF and TDDFT BNL off-site excitation energies are much higher than the other functionals and do in fact follow the Coulomb, $-R^{-1}$, dependence. In Figure 4, the off-site excitation energies for HF and BNL are compared to energies predicted by eq 7. The expression predicts that, upon breaking the symmetry through bond stretching, the two off-site energies remain quite similar. The TDHF and the TDDFT BNL energies are shown to be only slightly offset from the values predicted by eq 7. The other functionals greatly underestimate the off-site energies when compared to eq 7. Similarly, the BNL energies closely coincide with eq 8, where the differences between them are attributed to the symmetry-breaking effects on the BNL energies.

We also present the calculated energies upon symmetry breaking by a constant electric field of 0.1 V/Å applied perpendicular to the planes of the two parallel ethene molecules [see Figure 2 (left)]. The energy due to the electric field ($\pm E_f r$) is now added to eq 7, leading to

$$E_{CT} = \Delta\varepsilon_{orb} - \frac{1}{R} \pm E_f r \qquad (9)$$

Accordingly, one off-site excitation is stabilized and the other is destabilized by the field. We find that the LDA, PBE, and B3LYP off-site energies are again underestimated in comparison to eq 9. We also find that the off-site energy following the field direction is stabilized with increasing distance. This results from applying the same field over a larger distance, which amounts to an overall larger potential bias. The plotted eq 9 energies show that the Coulomb term (R^{-1}) is larger than the field term ($\pm E_f r$) at small dimer separation and therefore dominates. At large dimer separation, the $\pm E_f r$ term becomes dominant. The off-site energies of the pure density functionals are shown to depend only on the field term, as expected. Likewise, initially the B3LYP hybrid functional energies partially depend on the Coulomb term; however, the field term becomes dominant too quickly with increasing dimer separation. This spurious trend is eliminated in the case of the BNL functional, for which the evaluated off-site energies lie between the formal expression in eq 9 and the electrostatic interaction expression in eq 8, which includes the experimental IP and EA.

In the symmetric limit of the dimer system, the off-site excitations exhibit no net CT. At this limit, the B3LYP functional was shown above to fail (Figure 3). Indeed, conventional functionals greatly underestimate the off-site excitation energies, predicting energies lower than those of the on-site excitations (shown in Figure 5). A comparison between off-site excitation energies and corresponding orbital gaps also confirms the failure of the conventional functionals to incorporate the Coulomb distance dependence (shown in Figure 1 in Supporting Information). The HF and BNL off-site excitation energies are much higher than the on-site excitations, and they follow eq 7 until the dimer separation becomes small (also illustrated in Figure 1 in Supporting Information). TDHF fails at short dimer separations, as HF theory does not treat correlation effects. The BNL functional, on the other hand,

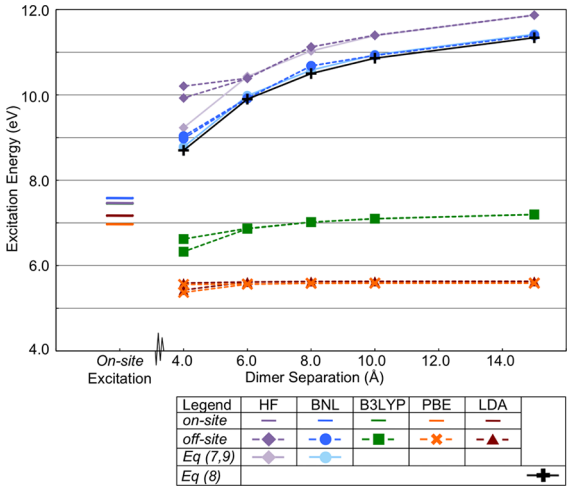

Figure 5. Excitation energies (in electronvolts) of the symmetric system. Off-site energies are compared to eq 7 and to eq 8, the long-range electrostatic interaction limit, where experimental IP and EA values are used. On-site energies for the 15 Å separation are included for comparison (Note: HF and B3LYP on-site state energies overlap).

treats both the correlation effects at short range and the Coulomb dependence at long range. It is important to note that both eq 7 and the off-site excitation energies for the BNL functional trace eq 8, essentially reproducing the "experimental trend". Therefore, the BNL functional is shown to produce accurate off-site excitation energies.

We next consider the vinylstilbene-functionalized octahedral silsesquioxanes (2-vinylstilbene−OHSQ) shown in Figure 6.

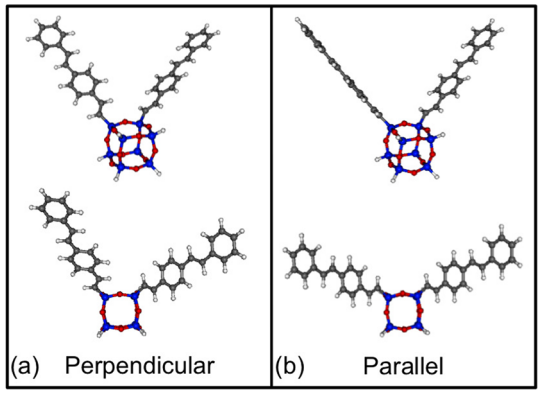

Figure 6. (a) Perpendicular and (b) parallel 2-vinylstilbene−OHSQ (top, side view; bottom, overhead view).

Recent experiments suggest the existence of CT (off-site) excitations in this system between the vinylstilbenes.[54,55] Although we have recently reported the importance of considering solvation effects on the CT state energy in such systems, here we only consider the off-site excitation energies in the gas phase.[65]

We consider two geometries of the 2-vinylstilbene−OHSQ molecule, where the vinylstilbene ligands are aligned either perpendicular (symmetry-broken) or parallel (symmetric) to each other, as illustrated in Figure 6. We used the B3LYP//6-31G* level of theory for geometry optimizations. For the TDDFT calculations, we used the 6-31G* and 6-31+G* basis sets, with the BNL and B3LYP functionals. It should be noted that the importance of including diffuse functions has

previously been shown.[57] The ground-state energies of the two structures differ by less than k_BT at room temperature, indicating that both are thermally populated at the ground state (ground-state energies are provided in Table 3 in Supporting Information). Similar to the ethene dimer, the low-lying excitations are on-site and off-site $\pi-\pi^*$ transitions.

We compare the parallel and perpendicular geometries in order to demonstrate the effect of symmetry breaking on the off-site excitation energies in the SQ-functionalized system. Figure 7 illustrates the detachment (hole) and attachment

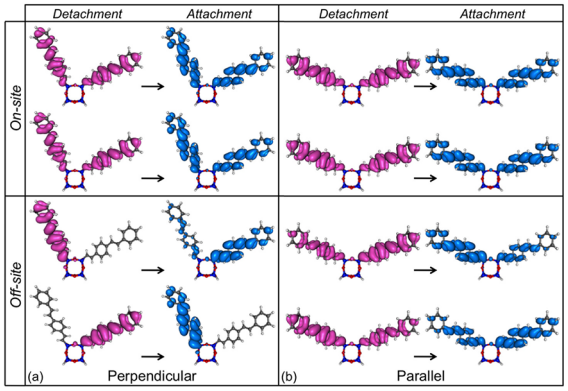

Figure 7. Detachment and attachment densities corresponding to on-site and off-site excitations for 2-vinylstilbene−OHSQ in the perpendicular and parallel geometries. The nondegenerate off-site excitations are localized on a single vinylstilbene in the perpendicular geometry and involve net CT. The degenerate off-site excitations are delocalized on both vinylstilbenes in the parallel geometry and involve significantly smaller net CT.

(electron) densities[69] corresponding to the on-site and off-site excitations. In the parallel (symmetric) geometry, the HOMO and LUMO orbitals are degenerate and therefore can be represented in the canonical MO basis as delocalized over both vinylstilbenes in the molecule, as shown in Figure 8. In the

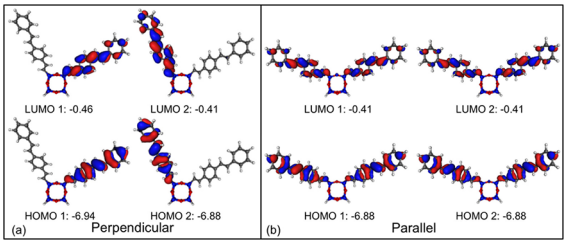

Figure 8. Orbital pictures and energies (in electronvolts) for 2-vinylstilbene−OHSQ structures. (Top) Perpendicular; nondegenerate orbitals are localized on each vinylstilbene. (Bottom) Parallel; degenerate orbitals are delocalized over both vinylstilbenes.

perpendicular (symmetry-broken) geometry, the orbital degeneracy is broken and each orbital is localized on a single vinylstilbene in the canonical MO basis. The orbital symmetry breaking also affects the net CT observed in the off-site excitations of 2-vinylstilbene−OHSQ. For instance, the off-site transitions exhibit minimal net CT in the parallel geometry and significant CT in the perpendicular geometry, as illustrated in Figure 7.

The $\pi-\pi^*$ excitation energies calculated with B3LYP and BNL are compared in Figure 9. Results obtained for both the 6-31G* and 6-31+G* basis sets are shown. The BNL on-site

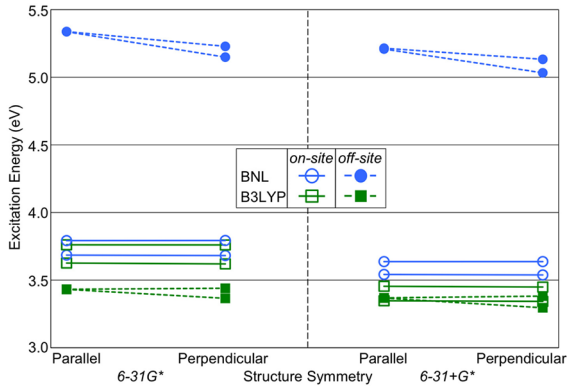

Figure 9. Excitation energies (in electronvolts) obtained for 2-vinylstilbene−OHSQ in the parallel and perpendicular geometries via TDDFT with B3LYP and BNL. Results obtained for the 6-31G* (left) and 6-31+G* (right) basis sets are shown.

energies are slightly higher than the B3LYP energies, and more so for the 6-31+G* basis set. The off-site excitations are less basis-set-dependent than the on-site excitations for the B3LYP functional. The B3LYP functional greatly underestimates the off-site excitation energies in accord with the TDDFT limitations discussed above. The RSH BNL functional correctly predicts the off-site excitation energies by correctly accounting for the electron−hole interaction and orbital gap. Importantly, even in the symmetric parallel case where there is minimal net CT, the BNL functional correctly identifies the off-site excitations as linear combinations of CT-type excitations.

5. CONCLUSIONS

Electronic states involving off-site excitations are not always characterized by net CT when the system is symmetrical. Nevertheless, standard DFT functionals such as B3LYP are still unable to account for the energies of such states. Furthermore, breaking the symmetry, and thereby giving rise to net CT, may improve the ability of the standard functionals to account for the energies of these states due to accidental cancellation of errors. In this paper, we demonstrate the accuracy and robustness of the BNL RSH functional for obtaining off-site excitations in both symmetric systems with zero net CT and asymmetric systems with net CT. We utilized a systematic symmetry-breaking scheme to determine the success of the BNL in treating off-site excitations in spatially separated dimer systems.

Indeed, the correct characterization of orbital gaps and CT character is particularly important in applications to OPV and OLED materials. In such systems, as exemplified by 2-vinylstilbene−OHSQ, multiple geometries with various symmetries can be populated at thermal equilibrium. Thus, robustness and accuracy of the BNL functional across geometries and symmetries make it particularly suitable for understanding CT in these systems.

■ ASSOCIATED CONTENT

Supporting Information

Four tables and two figures showing BNL γ parameters, ground-state energies, orbital energies, and correlation plots; and additional text with discussion on MO basis choice and net CT. This material is available free of charge via the Internet at http://pubs.acs.org.

AUTHOR INFORMATION

Corresponding Author

*E-mail eitan@umich.edu or bdunietz@kent.edu.

Present Address

[†]Department of Chemistry, Kent State University, Kent, OH.

Notes

The authors declare no competing financial interest.

ACKNOWLEDGMENTS

We thank Roi Baer for stimulating discussions and useful suggestions. B.D.D. gratefully acknowledges support by a DOE-BES award through the Chemical Sciences Geosciences and Biosciences Division (DE-SC0004924), DE-FG02-10ER16174. E.G. acknowledges that this work is pursued as part of the Center for Solar and Thermal Energy Conversion, an Energy Frontier Research Center funded by the U.S. Department of Energy Office of Science, Office of Basic Energy Sciences under 390 Award DE-SC0000957. H.P. acknowledges that this material is based upon work supported by the National Science Foundation graduate research fellowship under Grant DGE 0718128.

REFERENCES

(1) Coropceanu, V.; Cornil, J.; Filho, D. A. d. S.; Olivier, Y.; Silbey, R.; Bredas, J.-L. *Chem. Rev.* **2007**, *107*, 926−952.

(2) Günes, S.; Neugebauer, H.; Sariciftci, N. S. *Chem. Rev.* **2007**, *107*, 1324−1338.

(3) Forrest, S.; Thompson, M. *Chem. Rev.* **2007**, *107*, 923−925.

(4) Hagfledt, A.; Boschloo, G.; Sun, L.; Kloo, L.; Pettersson, H. *Chem. Rev.* **2010**, *110*, 6595−6663.

(5) Lo, S.-c.; Burn, P. L. *Chem. Rev.* **2007**, *107*, 1097−1116.

(6) Runge, E.; Gross, E. *Phys. Rev. Lett.* **1984**, *52*, 997−1000.

(7) Onida, G.; Reining, L.; Rubio, A. *Rev. Mod. Phys.* **2002**, *74*, 601−659.

(8) Burke, K.; Werschnik, J.; Gross, E. K. U. *J. Chem. Phys.* **2005**, *123*, 62206.

(9) Tozer, D.; Amos, R.; Handy, N.; Roos, B.; Serrano-Andres, L. *Mol. Phys.* **1999**, *97*, 859−868.

(10) Fabian, J. *Theor. Chem. Acc.* **2001**, *106*, 199−217.

(11) Liao, M.-S.; Lu, Y.; Scheiner, S. *J. Comput. Chem.* **2003**, *24*, 623−631.

(12) Magyar, R.; Tretiak, S. *J. Chem. Theory Comput.* **2007**, *3*, 976−987.

(13) Dreuw, A.; Head-Gordon, M. *J. Am. Chem. Soc.* **2004**, *126*, 4007−4016.

(14) Dreuw, A.; Weisman, J. L.; Head-Gordon, M. *J. Chem. Phys.* **2003**, *119*, 2943.

(15) Perdew, J.; Parr, R.; Levy, M.; Balduz, Jr. *J. Phys. Rev. Lett.* **1982**, *49*, 1691−1694.

(16) Sham, L.; Schluter, M. *Phys. Rev. Lett.* **1983**, *51*, 1888−1891.

(17) Perdew, J.; Levy, M. *Phys. Rev. Lett.* **1983**, *51*, 1884−1887.

(18) Janak, J. F. *Phys. Rev. B* **1978**, *18*, 7165−7168.

(19) Stein, T.; Eisenberg, H.; Kronik, L.; Baer, R. *Phys. Rev. Lett.* **2010**, *105*, 4−7.

(20) Tozer, D. J. *J. Chem. Phys.* **2003**, *119*, 12697.

(21) Kümmel, S.; Kronik, L. *Rev. Mod. Phys.* **2008**, *80*, 3−60.

(22) Seidl, A.; Görling, A.; Vogl, P.; Majewski, J.; Levy, M. *Phys. Rev. B* **1996**, *53*, 3764−3774.

(23) Baer, R.; Livshits, E.; Salzner, U. *Annu. Rev. Phys. Chem.* **2010**, *61*, 85−109.

(24) Hieringer, W.; Görling, A. *Chem. Phys. Lett.* **2006**, *426*, 234−236.

(25) Dreuw, A.; Head-Gordon, M. *Chem. Phys. Lett.* **2006**, *426*, 231−233.

(26) Hieringer, W.; Görling, A. *Chem. Phys. Lett.* **2006**, *419*, 557−562.

(27) The $\pi-\pi^*$ excitation corresponds to the 1b1u → 1b2g orbital transition for all functionals considered in this study. In the Hartree−Fock approximation, the 1b1u orbital is the HOMO; however, the 1b2g orbital is the LUMO + 4 instead of the LUMO (which has 4 Ag symmetry). This is a basis-set effect and does not occur when a smaller basis is employed, such as 6-31G*. For the conventional functionals in this study, the LUMO does possess 1b2g symmetry.

(28) Kuritz, N.; Stein, T.; Baer, R.; Kronik, L. *J. Chem. Theory Comput.* **2011**, *7*, 2408−2415.

(29) Richard, R. M.; Herbert, J. M. *J. Chem. Theory Comput.* **2011**, *7*, 1296−1306.

(30) Hirata, S.; Head-Gorden, M. *Chem. Phys. Lett.* **1999**, *314*, 291−299.

(31) Dreuw, A.; Head-Gordon, M. *Chem. Rev.* **2005**, *105*, 4009−4037.

(32) Hirata, S.; Head-Gordon, M.; Bartlett, R. J. *J. Chem. Phys.* **1999**, *111*, 10774.

(33) Leininger, T.; Stoll, H.; Werner, H.-J.; Savin, A. *Chem. Phys. Lett.* **1997**, *275*, 151−160.

(34) Iikura, H.; Tsuneda, T.; Yanai, T.; Hirao, K. *J. Chem. Phys.* **2001**, *115*, 3540−3544.

(35) Yanai, T.; Tew, D. P.; Handy, N. C. *Chem. Phys. Lett.* **2004**, *393*, 51−57.

(36) Tawada, Y.; Tsuneda, T.; Yanagisawa, S.; Yanai, T.; Hirao, K. *J. Chem. Phys.* **2004**, *120*, 8425−8433.

(37) Toulouse, J.; Savin, A.; Flad, H.-J. *Int. J. Quantum Chem.* **2004**, *100*, 1047−1056.

(38) Peach, M. J. G.; Cohen, A. J.; Tozer, D. J. *Phys. Chem. Chem. Phys.* **2006**, *8*, 4543−4549.

(39) Vydrov, O. A.; Scuseria, G. E. *J. Chem. Phys.* **2006**, *125*, No. 234109.

(40) Baer, R.; Neuhauser, D. *Phys. Rev. Lett.* **2005**, *94*, No. 043002.

(41) Livshits, E.; Baer, R. *Phys. Chem. Chem. Phys.* **2007**, *9*, 2932−2941.

(42) Henderson, T. M.; Janesko, B. G.; Scuseria, G. E. *J. Chem. Phys.* **2008**, *128*, No. 194105.

(43) Chai, J.-D.; Head-Gordon, M. *J. Chem. Phys.* **2008**, *128*, No. 084106.

(44) Weintraub, E.; Henderson, T. M.; Scuseria, G. E. *J. Chem. Theory Comput.* **2009**, *5*, 754−762.

(45) Stein, T.; Kronik, L.; Baer, R. *J. Chem. Phys.* **2009**, *131*, No. 244119.

(46) Stein, T.; Kronik, L.; Baer, R. *J. Am. Chem. Soc.* **2009**, *131*, 2818−2820.

(47) Epifanovsky, E.; Polyakov, I.; Grigorenko, B.; Nemukhin, A.; Krylov, A. I. *J. Chem. Theory Comput.* **2009**, *5*, 1895−1906.

(48) Lange, A.; Herbert, J. M. *J. Chem. Theory Comput.* **2007**, *3*, 1680−1690.

(49) Rohrdanz, M. A.; Herbert, J. M. *J. Chem. Phys.* **2008**, *129*, No. 034107.

(50) Rohrdanz, M. A.; Martins, K. M.; Herbert, J. M. *J. Chem. Phys.* **2009**, *130*, No. 054112.

(51) Mohammed, A.; Agren, H.; Norman, P. *Phys. Chem. Chem. Phys.* **2009**, *11*, 4439−4541.

(52) Pastore, M.; Mosconi, E.; Angelis, F. D.; Gratzel, M. *J. Phys. Chem. C* **2010**, *114*, 7205−7212.

(53) Sini, G.; Sears, J. S.; Bredas, J.-L. *J. Chem. Theory Comput.* **2011**, *7*, 602−609.

(54) Laine, R. M.; Sulaiman, S.; Brick, C.; Roll, M.; Tamaki, R.; Asuncion, M. Z.; Neurock, M.; Filhol, J.-S.; Lee, C.-Y.; Zhang, J.; Goodson, T.; Ronchi, M.; Pizzotti, M.; Rand, S. C.; Li, Y. *J. Am. Chem. Soc.* **2010**, *132*, 3708−3722.

(55) Sulaiman, S.; Bhaskar, A.; Zhang, J.; Guda, R.; Goodson, T.; Laine, R. M. *Chem. Mater.* **2008**, *20*, 5563−5573.

(56) Zhen, C.-G.; Becker, U.; Kieffer, J. *J. Phys. Chem. A* **2009**, *113*, 9707−9714.

(57) Phillips, H.; Zheng, S.; Hyla, A.; Laine, R.; Goodson, T.; Geva, E.; Dunietz, B. D. *J. Phys. Chem. A* **2012**, *116*, 1137−1145.

(58) Shao, Y.; et al. *Phys. Chem. Chem. Phys.* **2006**, *8*, 3172−3191.

(59) Dirac, P. A. M. *Proc. Cam. Philos. Soc.* **1930**, *26*, 376−385.
(60) Perdew, J.; Burke, K.; Ernzerhof, M. *Phys. Rev. Lett.* **1996**, *77*, 3865−3868.
(61) Becke, A. D. *J. Chem. Phys.* **1993**, *98*, 5648.
(62) Lee, C.; Yang, W.; Parr, R. G. *Phys. Rev. B* **1988**, *37*, 785−789.
(63) Vosko, S.; Wilk, L.; Nusair, M. *Can. J. Phys.* **1980**, *58*, 1200−1211.
(64) Stephens, P.; Devlin, F.; Chabalowski, C.; Frisch, M. *J. Phys. Chem.* **1994**, *98*, 11623−11627.
(65) Zheng, S.; Phillips, H.; Geva, E.; Dunietz, B. D. *J. Am. Chem. Soc.* **2012**, *134*, 6944−6947.
(66) Varetto, U. *Molekel 5.4.0.8*; Swiss National Supercomputing Centre, Manno, Switzerland.
(67) For BNL, as for HF, the 1b1u orbital is the HOMO, and the 1b2g orbital is the LUMO + 4, where the LUMO has 4 Ag symmetry. We compare the corresponding (1b1u−1b2g) orbital gap of the $\pi-\pi^*$ excitation to the fundamental gap, due to the significance of the IP and EA in transfer of an electron between ethene monomers. For reference, the BNL HOMO−LUMO gap, 11.2 eV, differs by only 1.1 eV from the fundamental gap, outperforming the conventional functionals considered in this study.
(68) Pearson, R. *Inorg. Chem.* **1988**, *27*, 734−740.
(69) Head-Gordon, M.; Grana, A. M.; Maurice, D.; White, C. A. *J. Phys. Chem.* **1995**, *99*, 14261−14270.